

# ACTINIDE CONVERSION CAPABILITIES OF MOLTEN SALT REACTORS (MSR)

L. MESTHIVIERS<sup>1</sup>, D. HEUER<sup>1</sup>, E. MERLE<sup>1</sup>, G. GRASSI<sup>2</sup>, B. MOREL<sup>2</sup>, G. SENENTZ<sup>2</sup>

<sup>1</sup>LPSC/IN2P3/CNRS, Grenoble INP, UGA, Grenoble, France

<sup>2</sup>Orano, Châtillon, France

Email contact of corresponding author: mesthiviers@lpsc.in2p3.fr

## Abstract

Currently operated French nuclear power plants mainly use enriched uranium. The used fuel is reprocessed to recover valuable materials, such as plutonium, which is recycled once in dedicated Pressurised Water Reactors (PWR) of the fleet. Once used, the quality of plutonium decreases and it becomes more difficult to recycle this plutonium in thermal spectrum reactors. The work presented in the article considers the use of low-quality plutonium in a concept of molten salt reactor (MSR) operated with a fast neutron spectrum and a chloride fuel. New studies have recently started as part of a CNRS/Orano collaboration to evaluate the efficiency and options of such an MSR to convert actinides, and specifically transuranic elements, into fission products to diminish the waste stockpile. This article provides some preliminary results. Neutronic, chemical and thermal-hydraulic constraints set the reactor configuration. Neutronic studies use a Monte-Carlo approach to calculate the burn-up, feedback coefficients, and irradiation damages in the axial and radial reflectors, whereas the design optimisation of the reactor fuel circuit is carried out with a thermohydraulic and neutronic correlation-based algorithm. The molten solvent considered in the calculations – NaCl-MgCl<sub>2</sub> – to incorporate plutonium has shown a neutronic impact according to the proportions of the two constituents. A large amount of magnesium tends to soften the spectrum, which is deleterious when considering non-fissile actinides. An observed increase of the irradiation damages on large core volumes is explained and the impact of reflectors to mitigate this effect through the mean neutron energy is presented. Finally, the paper shows that the calculated feedback coefficients are very good (around -17 pcm/K), which assures an excellent core stability and thus a good inherent safety. The ongoing studies thus demonstrate the promising potential of fast neutron chloride MSR for such applications, especially with small cores, leading to lower minor actinide production and displacements per atom.

## 1. INTRODUCTION

Uranium-based thermal-spectrum reactors produce plutonium and minor actinides (MAs), whose potential for reuse in the same kind of reactors is limited. Plutonium is currently recycled in dedicated light-water reactors (LWRs) only once due to the degradation of the isotopic quality of plutonium. Alternative solutions involving solid-fuel fast neutron spectrum reactors have been extensively studied over the past decades. We focus here on an innovative approach using a molten salt fast reactor.

The Molten salt reactors (MSRs) considered here are based on a liquid circulating fuel acting as a direct coolant in the heat exchangers. The liquid fuel considered for MSRs is based on a chloride (NaCl) or fluoride (LiF) solvent [1] where various heavy nuclei compositions can be dissolved. Thanks to this flexibility in the fuel composition, MSRs can be operated in both breeding or burning modes, with a thermal or fast neutron spectrum. Although burner MSR concepts have not been much studied until now, they may be of great interest for closing the fuel cycle.

In a fast-spectrum system, the fission over capture ratio is improved for all heavy nuclei, allowing most of the actinides to significantly fission. Therefore, a fast reactor concept is theoretically adapted to convert (i.e. fission) actinides such as plutonium. New studies are being carried out as part of a CNRS/Orano collaboration to evaluate the efficiency and options of MSRs as actinide converters. Even if minor actinides can also be converted, the present article focuses on the use of plutonium.

This paper first focuses on the configuration of the reactor in section 2 by looking at the neutronics, salt properties and thermal-hydraulic constraints.

In section 3, the intrinsic safety of the different reactor configurations for an operating period of 100 years to reach the steady-state is discussed, as well as the evolution of the different transuranic elements of interest. A

comparison of the material irradiation (displacement per atom) for the different reactor configurations is also presented.

## 2. REACTOR CONFIGURATION DEFINITION

### 2.1. Constraints from neutronics and salt properties

The new kind of MSR studied here aims at limiting transuranic elements build-up, by converting these elements into fission products. This goal implies specific constraints described in this paragraph, in terms of element solubility, and fuel temperature, volume and composition. In order to maximise the consumption of the transuranic elements, the solvent salt should have a good actinide solubility to optimise the ratio fuel / solvent. This has an impact on the reactor operating temperature: it should be low enough to avoid surrounding material damage during over-heating accident scenarios; but in case of over-cooling, plutonium and MA precipitation has to be avoided. A chlorine-based salt is therefore chosen for its high actinide (valence 3) solubility at reasonable operating temperatures. If a pure NaCl solvent salt is chosen – leading to a binary salt in the form of NaCl – PuCl<sub>3</sub> – the core volume, for a given core geometry, is imposed by the isotopic composition of the heavy elements to reach criticality, with no degrees of freedom left to adjust the fraction of heavy nuclei compared to NaCl. Different core volumes can only be obtained with multiple compositions. A solvent salt NaCl-MgCl<sub>2</sub> has thus been selected to gain an additional degree of freedom by playing on the proportion of MgCl<sub>2</sub>: in this way we can incorporate PuCl<sub>3</sub> fractions from 0 to 38.5% along the eutectic line at a fuel salt temperature of around 750 K. Using the ternary diagram on this salt [2], the eutectic line provides the composition for a given plutonium proportion and allows the reactor core volume to have any chosen size from approximately 80 litres to some tens of cubic meters.

Once the salt composition is set, the core volume is determined to reach criticality. An iterative Python programme coupled to MCNP (Monte-Carlo transportation code [3]) computes the critical core volume, using JEFF3.3 and ENDF/B-VII.1 nuclear data [4,5]. The evolution of the fuel salt density with the plutonium fraction is calculated with in-house data fitted from [6]. Thanks to this programme, the evolution of the critical core volume for different magnesium or plutonium proportions is established for each fuel type (Table 1), as only plutonium is considered here among the transuranic elements.

TABLE 1. ISOTOPIC MOLAR COMPOSITION OF THE PLUTONIUM-BASED FUELS (%) [7]

Isotopic composition	Pu ex-UOX	Pu ex-MOX
	BU 50GWj/t	BU 47GWj/t
	5-year cooldown	5-year cooldown
<sup>238</sup> Pu	3.1	4.2
<sup>239</sup> Pu	52.1	38.2
<sup>240</sup> Pu	25.2	32.4
<sup>241</sup> Pu	11.8	12.5
<sup>242</sup> Pu	7.8	12.7

Fig. 1 shows that the critical core volume increases for lower plutonium proportions with 50% of the fuel salt in the core. For a given plutonium proportion, if the plutonium quality decreases (PuU: Pu ex-UOX / PuM: Pu ex-MOX), the critical core volume increases. An MSR concept is very flexible as many different fuels can be used. As explained above, this flexibility is achievable by adjusting the magnesium proportion according to the plutonium quality.

Neutronics and salt properties set constraints on the reactor fuel circuit salt composition and volume. In addition, as the fuel also acts as coolant and circulates from the core to the primary heat exchangers to transfer its energy to the intermediate circuit, other constraints from thermohydraulics have also to be taken into account. This is described in the next paragraph.

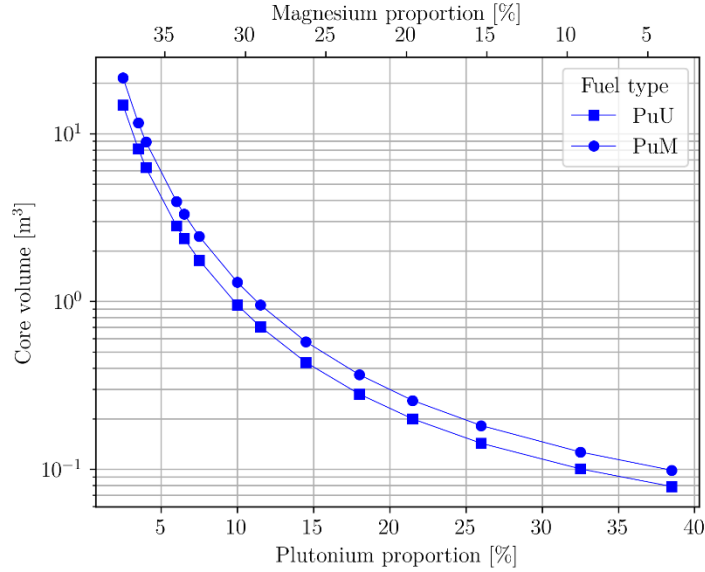


FIG. 1. Critical core volume evolution for different fuels

## 2.2. Thermohydraulic constraints

The fuel being liquid, the limit in terms of power density in the fuel is less restrictive. The fuel playing also the role of the coolant, it has to be able to evacuate the heat produced and the limit is on the heat exchanger side (pressure drops, heat transfer). The transferable energy is limited because of the heat exchanger design, its materials etc. One has also to watch out for the fuel salt velocity to avoid quick pipe corrosion. In order to have the best design, we used a homemade multicriteria optimisation code SONGE based on thermal-hydraulic correlations, with the recent addition of neutronic correlations thanks to the studies presented in section 2.1. Based on a genetic algorithm, this code employs user-input parameters and variables to optimise the fuel circuit design by minimizing the total cost on each variable [8]. We selected a CLiNaK salt for the intermediary loop (low melting point:  $\sim 580$  K) and set a margin of 30 K on each salt minimum temperature (core entrance for the fuel salt: min. 750 K, and corrugated plate heat exchanger entrance for the CLiNaK: min. 619 K). We chose to set the power density at  $150 \text{ MW}/\text{m}^3$  in this study but further optimisation shows that  $250 \text{ MW(th)}/\text{m}^3$  is achievable with 85 K in-core temperature increase and slightly more fuel salt outside of the core (60%).

## 3. REACTOR CHARACTERISTICS

This section summarises the characteristics of the reactor at the beginning of its operation (beginning of life) and for a considered operation time of 100 years to reach the steady-state for the fuel composition. It is to be noted that the reactor lifetime will be less than 100 years but the salt can be transferred in another unit and continue its composition evolution.

### 3.1. Beginning of Life calculations

#### 3.1.1. Fission efficiency

To evaluate the impact of the salt choice, different configurations are considered. The three main configurations are based on the geometry presented in Fig. 2 and described in Table 2. The top axial and radial reflectors are sliced to evaluate the atom displacement in the regions near the core. The ring radii of the axial reflector are equally separated and its  $n^{\text{th}}$  slice thickness is equal to  $2^n \cdot e_0$ . The radial reflector slices are also equally divided. For each design, different plutonium qualities are tested.

In order to effectively convert plutonium into fission products and avoid the build-up of heavier actinides, fission has to prevail over capture. Fig. 3 and 4 represent the fission-to-absorption ratios for each configuration according to equation (1):

$$r = \frac{\tau_f}{\tau_f + \tau_c} = \frac{\tau_f}{\tau_a} \quad (1)$$

where  $r$  is the proportion of fissions,  $\tau_f$  is the fission rate,  $\tau_c$  the capture rate and  $\tau_a$  the absorption rate.

TABLE 2. REACTOR CONFIGURATIONS

Characteristics	4% Pu		11.5% Pu		38.5% Pu	
	Pu ex-UOX	Pu ex-MOX	Pu ex-UOX	Pu ex-MOX	Pu ex-UOX	Pu ex-MOX
Core radius (m)	0.999	1.19	0.336	0.390	0.112	0.125
Core volume (m <sup>3</sup> )	6.27	8.93	0.71	0.95	0.079	0.098
Initial plutonium load (kg)	2620	3350	818	1105	252	315
Core power density (MW(th)/m <sup>3</sup> )	150					
Thermal power (MW(th)/)	939.75	1200	106.1	143.2	11.82	14.77
In-Core salt ratio	50%					
In-HX salt ratio	19.5%					
Radial reflector	Grade 316H (40 cm)					
Axial reflector	Grade 316H (1 m)					
Neutronic protection	B <sub>4</sub> C (10 cm)					
Fuel salt reprocessing	Solvent, uranium and transuranic elements are reinjected into the fuel salt					

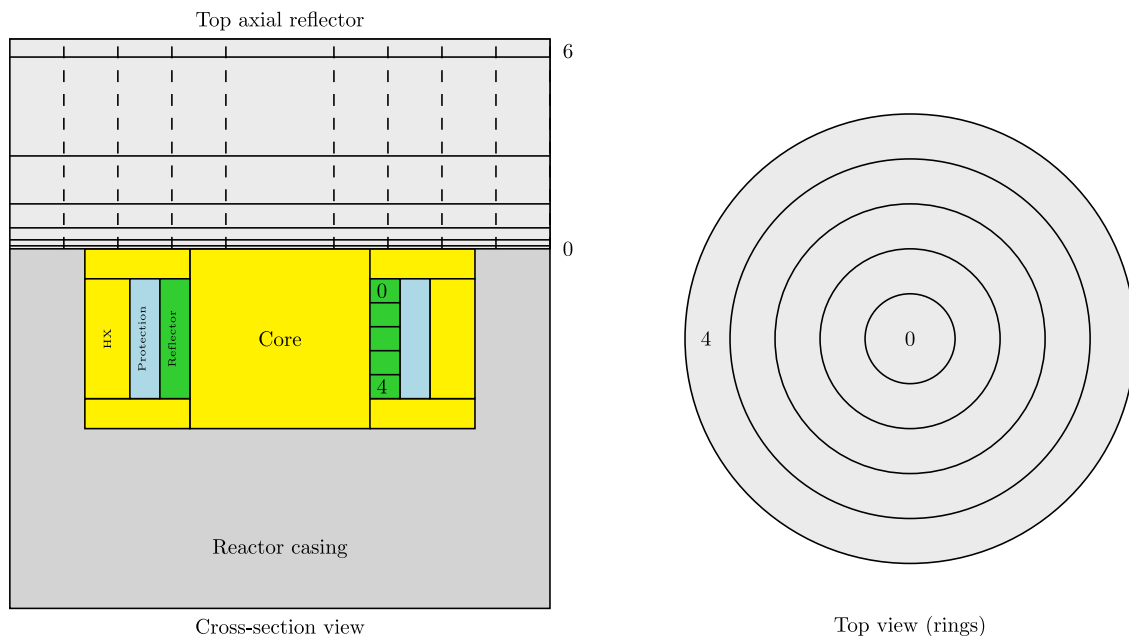


FIG. 2. Reactor design for the neutronic study of irradiation damages

Fig. 3 shows that fissions are favoured in small concepts and with good quality plutonium (ex-UOX). For larger cores, the plutonium proportion in the fuel salt decreases. The neutronic spectrum gets softer and fuel captures increase compared to fissions.

Fig. 4 highlights the fission proportions for the different plutonium isotopes. The trend shown in Fig. 3 is confirmed. Also, it is worth noting the large impact of the volume on the rate ratio for the  $^{240}\text{Pu}$  and  $^{242}\text{Pu}$  isotopes. To avoid the build-up of heavier actinides, small cores seem more suitable.

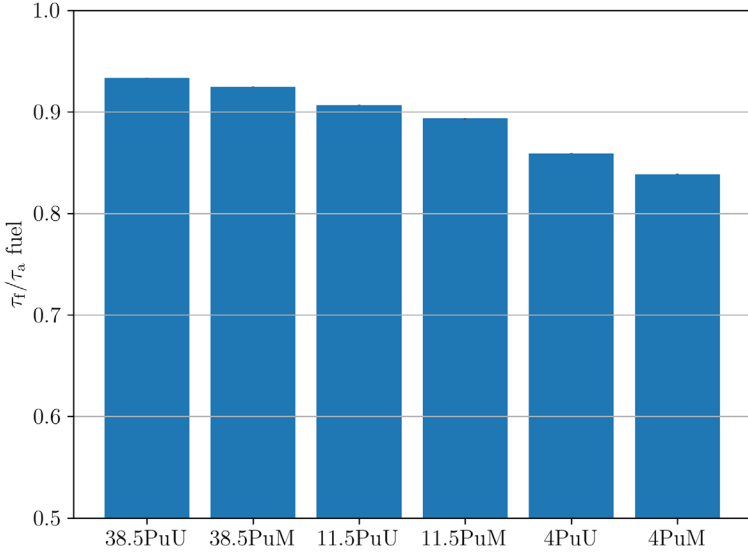


FIG. 3. Fission proportion for each configuration

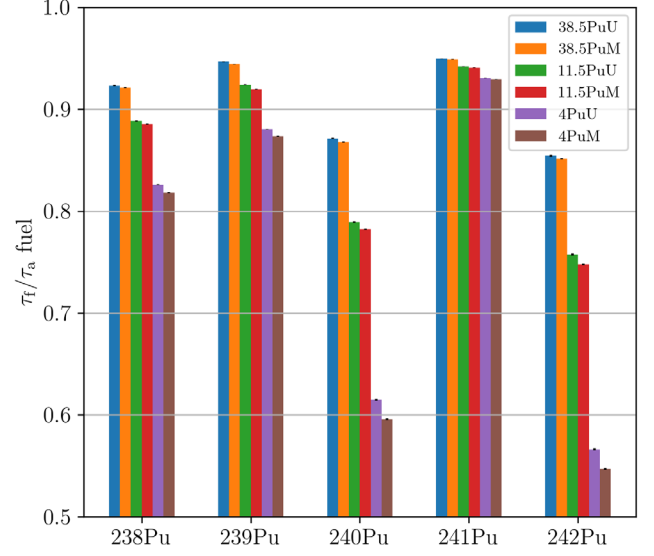


FIG. 4. Fission proportion for the different fuel isotopes

### 3.1.2. Feedback coefficients

Concerning the first safety function of reactivity control, the core of the reactor has to be intrinsically stable: this implies that the reactor has to autoregulate when diverting from the nominal operating temperature thanks to the thermal feedback effects. Two main physical phenomena do this regulation in the circulating fuel salt of MSR: the Doppler and the density effects. The Doppler effect is a spectrum phenomenon on the resonances, which broaden when the temperature rises, boosting capture over fission, and vice versa. The density effect comes from a decrease of fissile material volumetric concentration in the core due to salt dilatation. When the fuel dilates, the density decreases, the fuel is more transparent to neutrons, and more neutrons escape the reactor without inducing fissions. To allow salt dilatation (and reduce fissile material in the reactor), part of the salt is driven into a free level of the fuel circuit. To be stable in any situation, the reactor must have negative feedback coefficients. To evaluate these coefficients, the density and temperature of the fuel salt are individually modified around their reference values, see equations (2) and (3).

$$FC_{\text{Doppler}} = f(\rho_{\text{ref}}, T) \quad (2)$$

$$FC_{\text{density}} = f(T_{\text{ref}}, \rho(T)) \quad (3)$$

where  $FC_{\text{Doppler}}$  is the Doppler feedback coefficient,  $FC_{\text{density}}$  is the density feedback coefficient,  $\rho_{\text{ref}}$  is the reference density,  $T$  is the mean temperature of the fuel salt,  $T_{\text{ref}}$  is the reference mean temperature and  $\rho(T)$  is the fuel salt density at a given temperature  $T$ .

The density evolution is assumed to be linear with temperature, and both thermal dilatation coefficient and initial density depend on the actinide and magnesium fractions and are computed with the ionic volume of the fuel salt and reference salts from [6].

The operating – and reference – temperature is set at 800 K for neutronic studies, high enough from the melting point of the ternary salt to prevent solidification in case of over-cooling. The mean fuel salt density and Doppler feedback coefficients are computed from the evolution of the  $k_{\text{eff}}$  around 800 K, from 750 K to 1000 K, with a logarithmic regression for the Doppler effect and a 2<sup>nd</sup> order polynomial for the density effect considering the statistical uncertainties on the computed  $k_{\text{eff}}$  with JEFF3.3.

In Fig. 5, the larger the reactor volume, the lower the density feedback coefficient ( $-18; 16.3 \text{ pcm/K}$  at  $800 \text{ K}$ ). When the fuel salt leaves the core due to dilatation, the change in the neutron leaks is more important for small configurations. In Fig. 5, the Doppler feedback coefficients are much smaller in absolute value ( $-0.7; -0.1 \text{ pcm/K}$  at  $800 \text{ K}$ ) and do not consider uncertainties on the cross-section databases, which could lead to a null Doppler effect on some designs. The Doppler effect being a competition between capture and fission resonances, it is more favourable for large cores as the spectrum is softer and neutrons are more likely to be captured in the resonances of the fuel. It is to be noted that  $^{239}\text{Pu}$  and  $^{240}\text{Pu}$  are responsible for almost all of the effect and the solvent ( $\text{NaCl-MgCl}_2$ ) shows no impact whatever the configuration. Some feedback coefficients have also been computed with ENDF/B-VIII.0 to estimate the impact of the cross-section library used. They have shown low influence on the results as shown in Table 3.

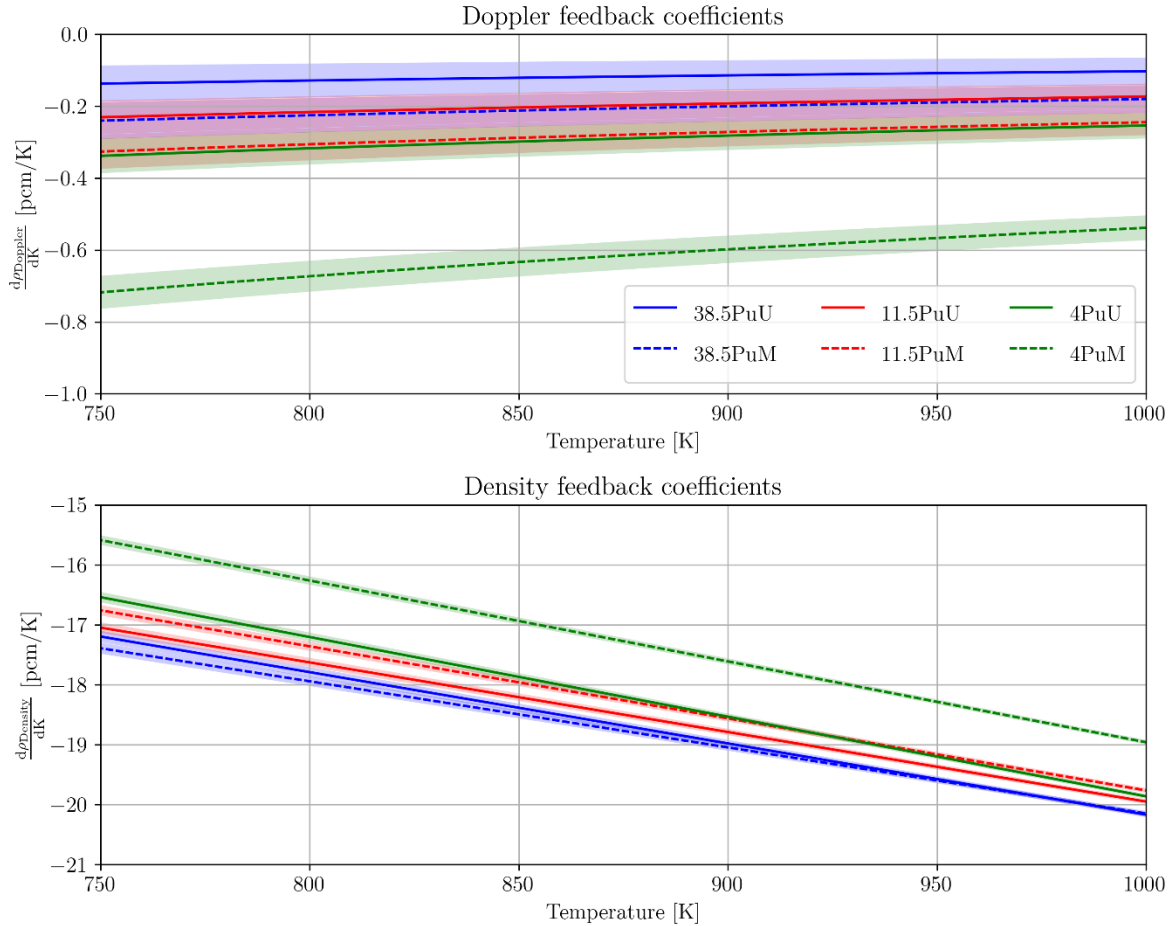


FIG. 5. Evolution with the temperature of the fuel salt Doppler and density feedback coefficients (only statistical error shown)

TABLE 3. COMPARISON OF THE FEEDBACK COEFFICIENTS AT  $800 \text{ K}$  FOR JEFF 3.3 AND ENDF/B-VIII.0 (UNIT IN  $\text{PCM/K}$ )

Configuration	4% Pu ex-MOX		4% Pu ex-UOX		11.5% Pu ex-UOX	
	Doppler	Density	Doppler	Density	Doppler	Density
JEFF 3.3	-0.67	-16.27	-0.32	-17.21	-0.22	-17.63
	$\pm 0.04$	$\pm 0.07$	$\pm 0.04$	$\pm 0.07$	$\pm 0.04$	$\pm 0.08$
ENDF/B-VIII.0	-0.63	-16.47	-0.47	-17.26	-0.26	-17.65
	$\pm 0.04$	$\pm 0.07$	$\pm 0.04$	$\pm 0.07$	$\pm 0.05$	$\pm 0.08$

### 3.2. Depletion calculation

Once assured that the reactor is stable at the beginning, the in-house CNRS evolution code REM [9,10] coupled with MCNP computes the evolution of the materials in the core – fuel, reflectors, etc. – and maintains the criticality at the operating temperature thanks to the injection of fresh fuel. A full description of the fuel reprocessing units can also be added to follow the fuel salt composition evolution out of flux: gas, insoluble elements and fuel salt have their own reprocessing scheme. In the calculations presented here, the reprocessing units extract all elements except the solvent NaCl-MgCl<sub>2</sub>, uranium and transuranic elements.

#### 3.2.1. Ionic volume

Because of fresh fuel injection, reprocessing, and nuclear and chemical reactions, the volume of the fuel salt changes over time. It is therefore needed to monitor its evolution during the simulation. An approximation of the real volume is computed with the ionic radii of all the elements in the fuel salt. The aim is to limit the volume change to 1-2%. To achieve this, an iteration process using a dichotomy is manually carried out by adjusting the fuel extraction time on each simulation until the 1% variation is met. Fig. 6 shows that the evolution of the volume is limited to 2% maximum, which is satisfying, for a complete cleaning time of 18.3 years. The settings of the fuel reprocessing unit are therefore acceptable.

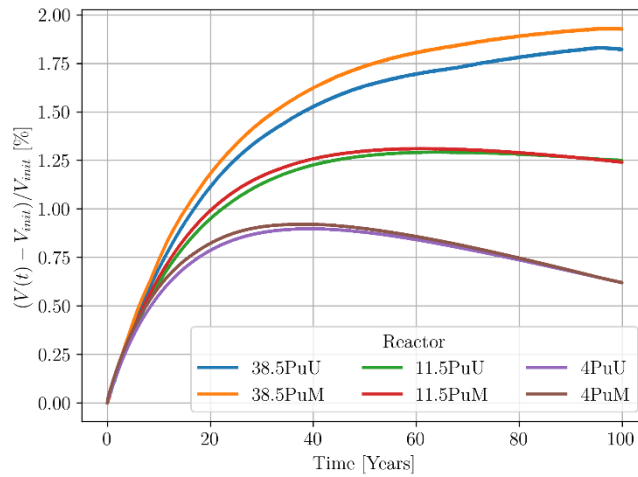


FIG. 6. Relative ionic volume ratio for the different configurations

#### 3.2.2. Inventory evolution

##### (a) Overall actinide evolution.

Fig. 7 and 8 show the time evolution of the three main actinides in the fuel salt for the plutonium ex-UOX- and ex-MOX-based reactors. A normalisation over the molar composition of the actinides has been carried out to compare the three main configurations, whose initial plutonium proportion differs consequently (38.5, 11.5 and 4%). The plutonium proportion is rather constant, even if slightly decreasing over the years. For the three designs in both figures, the americium proportion stabilises around the same value (3-4%). However, the ratio americium/curium differs significantly from a configuration to another. The larger the core, the higher the curium production. This is explained by the higher capturing rate for low plutonium concentration salts – i.e. large cores – as shown in Fig. 3.

##### (b) Isotopic evolution.

The evolution of the plutonium isotopic composition is drastically different when looking at the different configurations. Fig. 9 and 10 show the time evolution of the plutonium isotopic composition for the 38.5% and 4% plutonium-based salts, for the two types of plutonium (Pu ex-UOX and Pu ex-MOX). As expected from the

fission/absorption rate, the small reactor configuration limits the production of even nuclei, whereas their production is boosted in the 4% Pu-based configuration. It is to be noted that the 11.5% plutonium-based configuration, not shown here, shows an intermediary evolution of the isotopic composition.

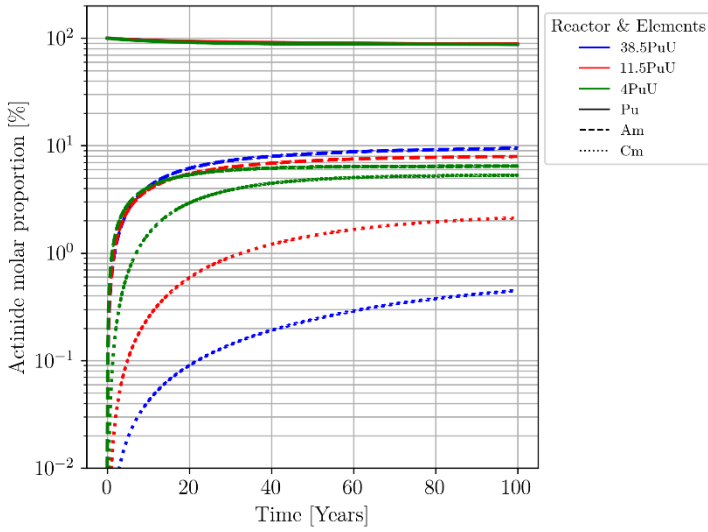


FIG. 7. Actinide molar proportion evolution for the PuU-based reactors

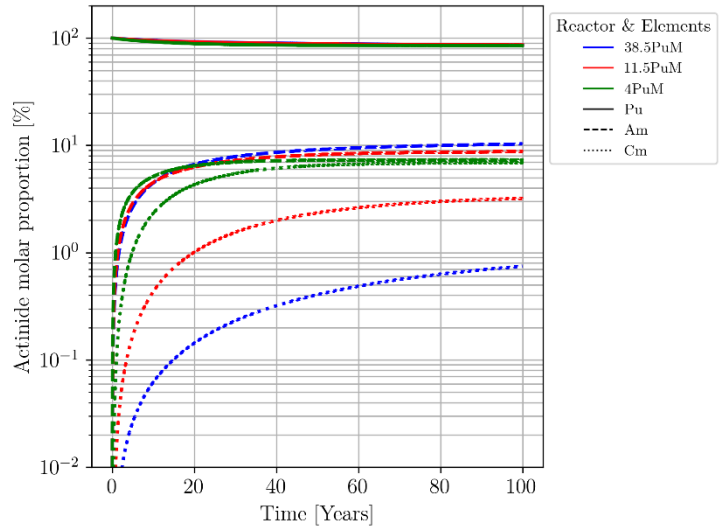


FIG. 8. Actinide molar proportion evolution for the PuM-based reactors

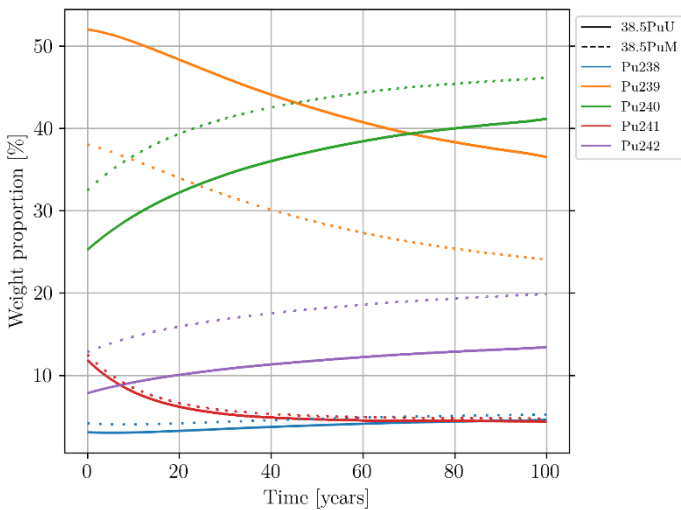


FIG. 9. Evolution of the plutonium isotopic composition in the 38.5%Pu configuration

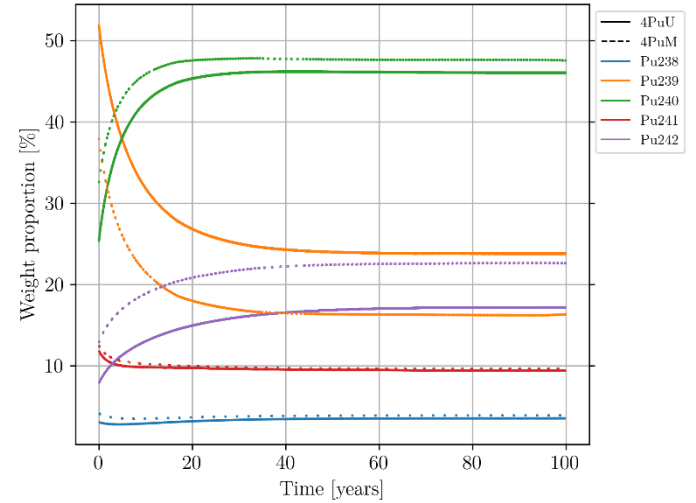


FIG. 10. Evolution of the plutonium isotopic composition in the 4%Pu configuration

### 3.2.3. Thermal feedback coefficient evolution

As shown in Fig. 5, the density feedback coefficients are very negative whereas the Doppler effect is small at the beginning of life of the reactors. Fig. 11 shows the evolution of the Doppler and density feedback coefficients over time for the different reactor configurations. The Doppler effect tends to diminish and get close to zero. The same evolution is observed for the density effect. Part of the evolution can be explained for the small configurations by the evolution of the thermal dilatation coefficient. Indeed, as the fractions of magnesium and actinides change with time, the thermal dilatation coefficient becomes stronger [+8% for the 4%Pu, +7% for the 11.5Pu and +2% for the 38%Pu configurations]. For the medium and big cores, the evolution of the density and the composition could result in decreasing leaks and reduce the feedback coefficient.



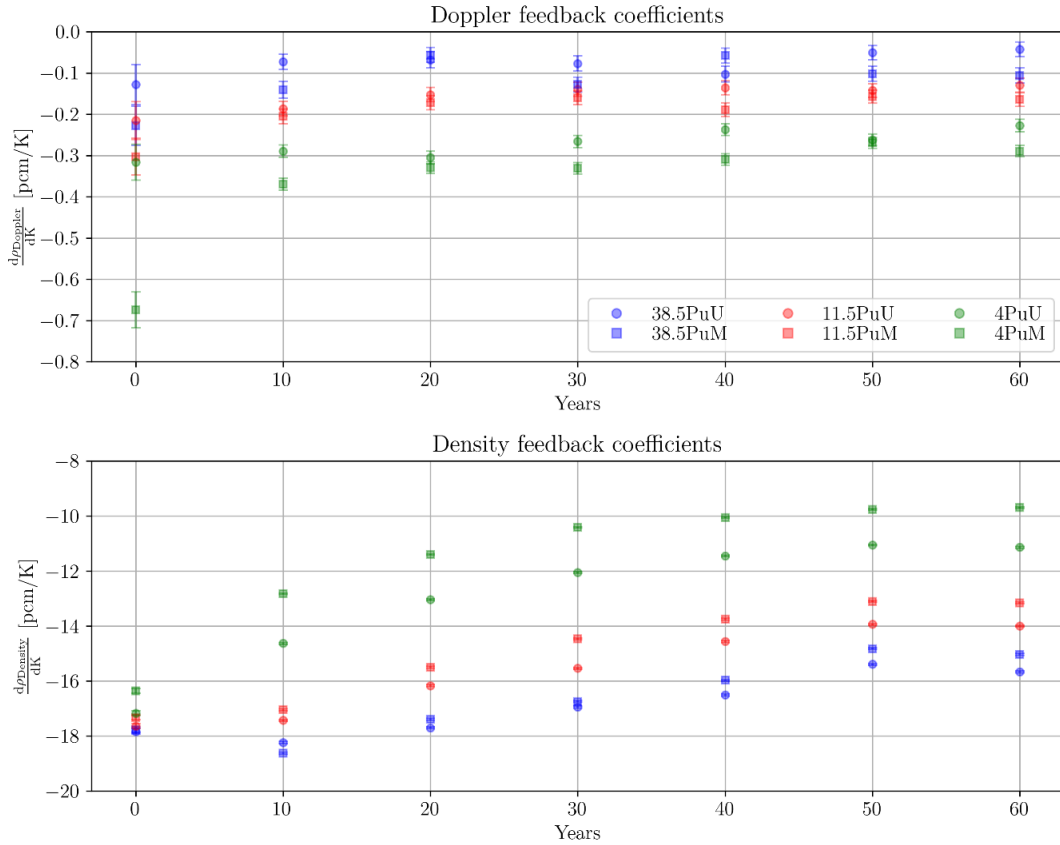


FIG. 11. Time evolution of the mean feedback coefficients

### 3.2.4. Radioisotope production

Because the mean free path of the neutrons in the reactor is large (fast spectrum), captures occur not only in the fuel but also in all the elements composing and surrounding the fuel salt. This leads to activation products. The use of a chlorine<sup>1</sup>-based salt induces  $^{36}\text{Cl}$  production by  $(n, \gamma)$  reaction on  $^{35}\text{Cl}$  and  $(n, 2n)$  reaction on  $^{37}\text{Cl}$ . An enrichment of natural chlorine in  $^{37}\text{Cl}$  may be considered to significantly reduce  $^{36}\text{Cl}$  production (volatile and long-lived radioisotope) and its impact on waste. A 100%  $^{37}\text{Cl}$  enrichment is used in the simulation for preliminary results. Fig. 12 shows the production of  $^{36}\text{Cl}$  over time for the different configurations. It is to be noticed that chlorine is not extracted in the reprocessing unit as it composes the salt solvent. To compare the different configurations, the  $^{36}\text{Cl}$  production is here shown by thermal power unit. For the first 40 years of operation, a clear trend is visible: The larger the reactor, the higher the  $^{36}\text{Cl}$  production by unit of thermal power. However, for the two largest cores, the  $^{36}\text{Cl}$  production slows down. Under the hypothesis of a 100%  $^{37}\text{Cl}$ -enriched solvent, the main production of  $^{36}\text{Cl}$  is due to the  $(n, 2n)$  reaction, which occurs at a threshold energy of 10.6 MeV [11,4]. As the neutron mean energy decreases with the increasing volume – softer neutron spectrum – the  $^{36}\text{Cl}$  production stabilises more quickly for low plutonium-based salt proportions. Sulphur production via  $[(n, \alpha) + \text{decay}]$  reaction on both  $^{35}\text{Cl}$  and  $^{37}\text{Cl}$  should be as limited as possible, as sulphur could increase the corrosion of the structural elements despite its extraction during the fuel salt reprocessing. Fig. 13 shows its concentration in the fuel salt for the different fuel types and sizes. Large cores with recycled plutonium tend to more concentrate sulphur, due to the softer spectrum inducing more captures on the chlorine nuclei.

<sup>1</sup> Natural chlorine composition: 75.76%  $^{37}\text{Cl}$ , 24.24%  $^{35}\text{Cl}$

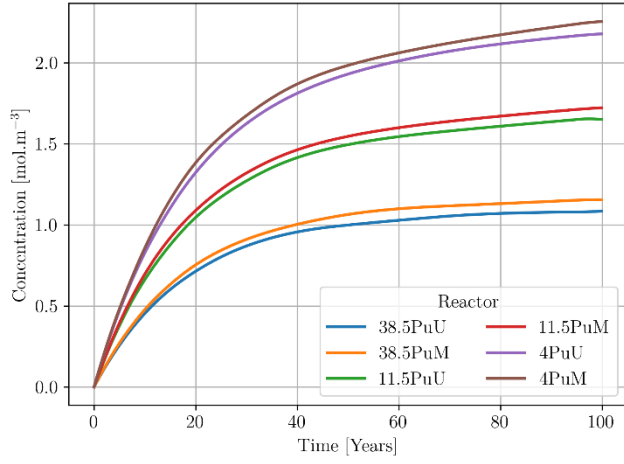
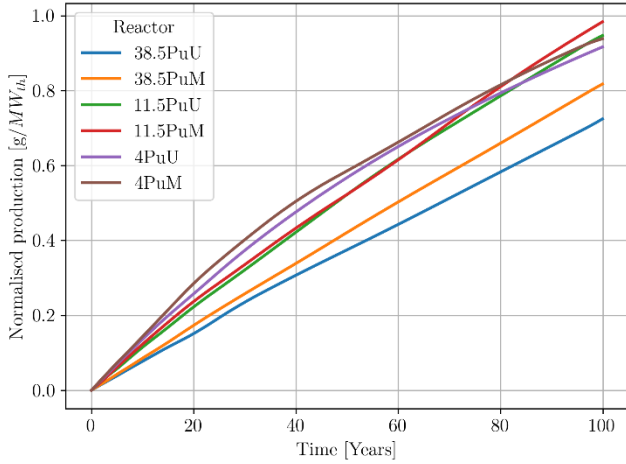


FIG. 12.  $^{36}\text{Cl}$  production for the different reactor configurations

FIG. 13. Sulphur concentration for the different reactor configurations

### 3.2.5. Irradiation damage

The MSR concept presented in this article is a fast spectrum reactor, hence leading to larger damages of the structures surrounding the core than a thermal spectrum. To assess the damages and evaluate the frequency of the maintenance needed to replace some parts, DPA (displacements per atom) calculations have been performed. The radial and top axial reflectors are subdivided in small volumes to identify the most impacted regions (Fig. 2). The radial reflector is 40 cm thick but only the first centimetre next to the core is cut into 5 equally distributed slices, as we checked for other MSFR configurations that the most irradiated material is logically close to the core.

The core power distribution in the core is axially and radially symmetrical as shown in Fig. 14 and 15 for the 38.5% PuU reactor. Both axially and radially, the maximum of the irradiation is located in the centre and close to the core (ring and slice 0 for the axial reflector, slice 2 for the radial reflector). To be easily removable, the reflectors could be built in several layers, stacked on each other.

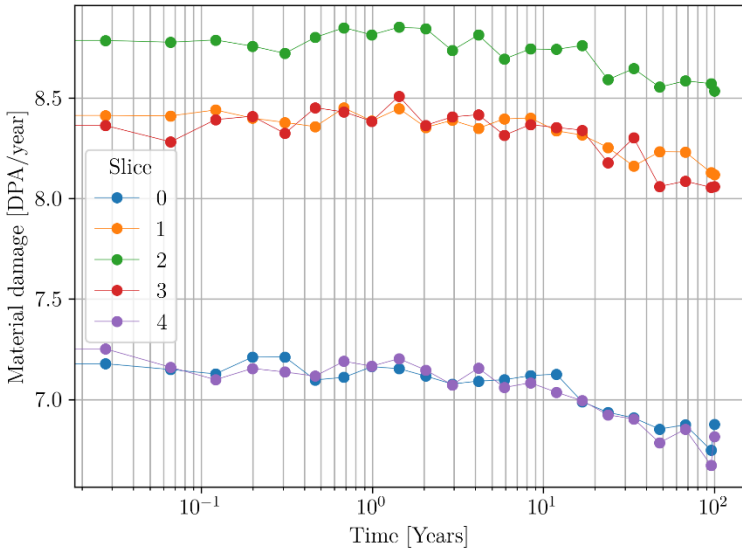


FIG. 14. Temporal DPA evolution in the radial reflector in the 38.5% PuU reactor

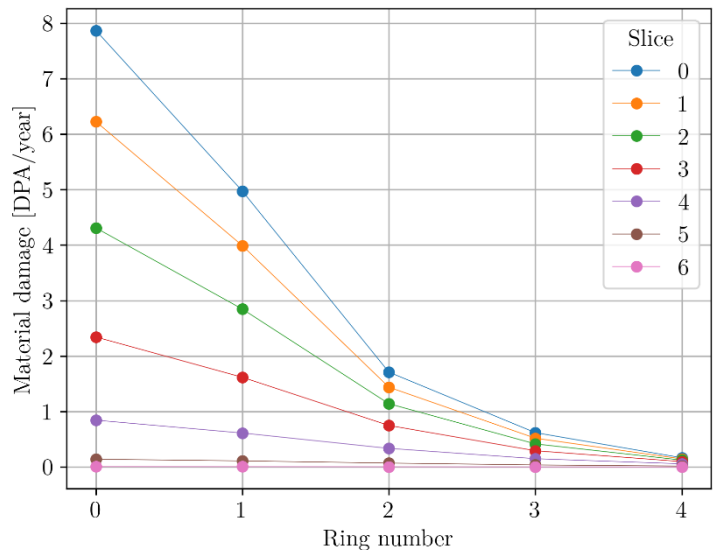


FIG. 15. Maximum DPA in the top axial reflector in the 38.5% PuU reactor

The atom displacement increases with the volume, as shown in Fig. 16. Indeed, the reactor power is proportional to the core volume and induces the neutron emission flux. The scalar flux on the core walls is proportional to the radius and power density – the latter being identical for all reactor configurations in this study. However, the effect is not linear, as the mean energy of the neutron population in the reflectors decreases. The proportion of plutonium in the fuel salt diminishes with the volume and the salt neutronic spectrum softens. It is

to be noted that the mean DPA in the first slice of the top axial reflector is slightly smaller for Pu ex-MOX fuel than Pu ex-UOX fuel, though having larger cores.

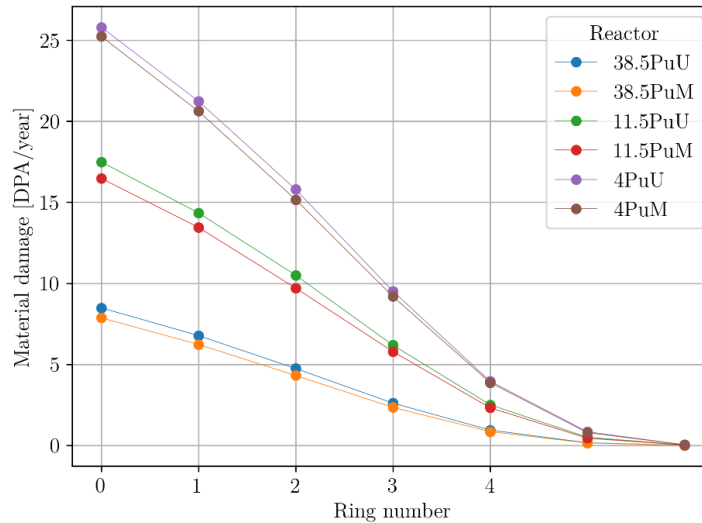


FIG. 16. Evolution of the atom displacement (DPA) in the first slice in the top axial reflector for different reactor configurations

#### 4. CONCLUSIONS

Different configurations of MSR aiming at converting plutonium produced in LWRs have been studied. The first part of the article explained the neutronic, chemical and thermal-hydraulic constraints considered to set the reactor configuration. Then calculations have been presented to characterize the initial state (beginning of life) of the MSR considered, in terms of fission efficiency and thermal feedback coefficients. Finally, depletion studies have been performed to evaluate the variation of the fuel composition, the production of specific radioisotopes, the irradiation damages (DPA), and the variation of the feedback coefficients. In particular, result shows that feedback coefficients are very good (negative values), ensuring the core stability and thus the intrinsic safety of the system. However, the small Doppler effect advocates for further studies on the dynamic of the reactor (filling, reactivity transient).

From the studies, high plutonium proportions – small cores – seem better in terms of irradiation damage, radioisotope and heavy nuclei production. Furthermore, the use of Pu ex-UOX or ex-MOX has a small impact on the different characteristics on small cores. On larger cores, Pu ex-MOX reactor configurations see fewer irradiation damages but higher minor actinide production. The results presented here show the potential of those reactors for converting plutonium. These also advocate further studies on the use of small reactors and/or the conversion of minor actinides that may be of great interest and suitable for the applications considered in this paper. Also, safety studies of such reactors have to be performed to confirm their potentiality. Finally, scenario studies for the deployment of such reactors are crucial to estimate their impact in terms of efficiency and effectiveness, in accordance with countries' needs and goals.

#### ACKNOWLEDGEMENTS

The authors wish to thank the NEEDS (Nucléaire: Energie, Environnement, Déchets, Société) French program, the IN2P3 department of the National Centre for Scientific Research (CNRS) and Grenoble Institute of Technology for their support. Finally, the authors are also thankful to Michel Allibert and Axel Laureau for their explanations and support.

#### REFERENCES

[1] MSR concept overview, Generation IV Forum. Visited on 31/05/2021. [https://www.gen-4.org/gif/jcms/c\\_42150/molten-salt-reactor-msr](https://www.gen-4.org/gif/jcms/c_42150/molten-salt-reactor-msr)

- [2] BENEŠ, O., KONINGS, R. J. M., Thermodynamic evaluation of the NaCl–MgCl<sub>2</sub>–UCl<sub>3</sub>–PuCl<sub>3</sub> system, *Journal of nuclear materials* 375.2 (2008): 202-208
- [3] BROWN, F. B., et al., MCNP version 5, *Trans. Am. Nucl. Soc.*, 87- 273 (2002): 02-3935
- [4] PLOMPEN, A.J.M, et al., The joint evaluated fission and fusion nuclear data library, JEFF-3.3, *Eur. Phys. J. A* 56 (2020): 181
- [5] CHADWICK, M.B., et al., ENDF/B-VII.1: Nuclear Data for Science and Technology: Cross Sections, Covariances, Fission Product Yields and Decay Data, *Nuclear Data Sheets* 112 (2011): 2887
- [6] JANZ, G. J., et al., Molten salts: Volume 4, part 2, chlorides and mixtures—electrical conductance, density, viscosity, and surface tension data, *Journal of Physical and Chemical Reference Data* 4, 871 (1975)
- [7] VIDAL, J., ESCHBACH, R., LAUNAY, A., et al., CESAR5.3: an industrial tool for nuclear fuel and waste characterization with associated qualification, WM2012, Phoenix Arizona (2012)
- [8] LAUREAU, A., LORENZI, S., MERLE, E, et al, SAMOFAR (A Paradigm Shift in Nuclear Reactor Safety with the Molten Salt Fast Reactor), European project, Work-Package WP1, Deliverable D1.3, Grant Agreement number: 661891 (2017)
- [9] DOLIGEZ, X., et al., Coupled study of the Molten Salt Fast Reactor core physics and its associated reprocessing unit, *Annals of Nuclear Energy* 64 (2014): 430–440
- [10] MERLE-LUCOTTE, E., et al., Simulation Tools and New Developments of the Molten Salt Fast Reactor, Contribution A0115, Proceedings of European Nuclear Conference ENC2010, Barcelona, Spain (2010)
- [11] SOPPERA, N., BOSSANT, M., DUPONT, E., JANIS 4: An Improved Version of the NEA Java-based Nuclear Data Information System, *Nuclear Data Sheets* 120 (2014): 294-296